

1 Flood discharge measurement of a mountain river – Nanshih River in Taiwan

2

3 Yen-Chang Chen¹4 ¹ Associate Professor, Department of Civil Engineering, National Taipei University of

5 Technology, Taipei, Taiwan, Tel: +886-2-27712171 ext. 2639; Fax: +886-2-27814518; E-mail:

6 yenchen@ntut.edu.tw.

7

8 Abstract

9 An efficient method that accounts for personal safety, accuracy and reliability for
10 measuring flood discharge of the Nanshih River at the Lansheng Bridge is proposed. The
11 method applying available tools which are adapted for flood conditions can be used to
12 quickly and accurately measure flood discharge. Measuring flood discharge directly from
13 mountain rivers by using conventional discharge measurement methods is costly,
14 time-consuming, and dangerous. Thus previous discharge estimations for mountainous area
15 in Taiwan were typically based on indirect methods, which alone cannot generate accurate
16 measurements. This study applies a flood discharge measurement system composed of an
17 Acoustic Doppler Profiler and crane system to accurately and quickly measure velocity
18 distributions and water depths. Moreover, an efficient method for measuring discharge, which
19 is based on the relationship between mean and maximum velocities and the relationship

20 between cross-sectional area and gauge height, is applied to estimate flood discharge. Flood
21 discharge of the Nanshih River at the Lansheng Bridge can be estimated easily and rapidly by
22 measuring maximum velocity in the river cross-section and the gauge height. The measured
23 flood discharges can be utilized to create a reliable stage-discharge relationship for
24 continuous estimations of discharge using records of water stage. Results of measured
25 discharges and estimated discharges of the Nahshih River at the Lansheng Bridge only
26 slightly differed from each other, demonstrating the efficiency and accuracy of the proposed
27 method.

28

29 **1. Introduction**

30 Discharge data enable populations to share and manage finite water supplies. Effective
31 water management requires accurate discharge measurements. With an average annual
32 precipitation of 2,471 mm, rainfall is abundant in Taiwan. Thundershowers and the typhoons
33 bring heavy downpours in the summertime. Therefore, the distribution of rainfall is uneven,
34 making the water available for use per capita low. As water shortages become increasingly
35 apparent, accurate discharge measurements become crucial. Sources of all major rivers
36 worldwide are located in mountains and a significant proportion of the earth's surface is
37 mountainous. Mountain rivers supply a large share of the world's population with fresh
38 water (Viviroli and Weingartner, 2004). A mountain river is a river located within a

39 mountainous region and has a stream gradient greater than or equal to 0.2% (Jarrette, 1992)
40 along the majority of its channel-length. Mountains cover about 27% of the world's land
41 surface, but only 13% of mountainous rivers have data (Bandyopadhy et al., 1997).
42 Although the World Meteorological Organization recommends using high-density
43 instrument networks in mountainous areas, the number of stream-gauging stations is still far
44 lower than the recommended number (WMO, 1988). With a total area of about 36,179 km²,
45 two-thirds of Taiwan is covered with forested peaks. Steep mountain terrain above 1,000 m
46 elevation constitutes about 32 % of the island's land area; hills and terraces between 100 and
47 1,000 m above sea level make up 31 %. However only a few of gauging stations can be
48 found in Taiwan's mountain area. The reasons accounting for the lack of data for mountain
49 rivers discharges are lack of funding, limitations of conventional methods and instruments
50 for discharge measurement, difficulties in accessing gauging stations, and harsh
51 environments that hinder discharge measurements.

52 A mountain river is a river located within a mountainous region and has a stream
53 gradient greater than or equal to 0.2% (Jarrette, 1992) along the majority of its
54 channel-length. Understanding the temporal and spatial variability of mountain river
55 hydrology requires measuring discharge directly, systematically, and periodically. The most
56 popular conventional method (current-meter method) for directly measuring discharge first
57 measures velocities and cross-sectional areas. The required velocity measurements are

58 obtained by placing a current meter at a desired location. However, during rapid flows
59 associated with floods, submerging a meter in water is almost impossible, even when an
60 adequate sounding weight is utilized. Additionally, riverbed instability due to rapid scouring
61 and deposition during flooding make sounding water depth impossible; thus, measuring a
62 cross-sectional area is extremely difficult. Flow conditions during floods are highly
63 unsteady and water stages and discharges vary dramatically. Thus, accurate discharge
64 measurements must be completed quickly. Furthermore, the conditions when measuring
65 mountain river discharge during floods are far from ideal, especially as floods often occur
66 during thundershowers and typhoons in Taiwan. Heavy rains and rapid flows combined with
67 threats to the safety of hydrologists and instruments add to the difficulties associated with
68 accurate measurements. Consequently, discharge data for mountain rivers are lacking in
69 Taiwan. Due to these unsuitable conditions, using a velocity meter to measure discharge is
70 difficult at best. Some new monitoring systems apply fixed side-looking Doppler profilers
71 (H-ADCP) to measure river discharge (Nihei and Kimizu, 2008; Le Coz et al., 2008).
72 However the water depth of the mountain rivers is usually very shallow. Intense rainfall
73 events are frequent enough to cause significant high concentrations of suspended sediment
74 in rivers that can also limit the function of ADCP. Those expensive systems lie idle most of
75 the time. However it is possible to install an H-ADCP at an ideal site to measure high flow.
76 A non-contact method that uses such instruments as a float (ISO, 2007; Rantz, 1982), optical

77 current meter (Bureau of Reclamation, 1997), radar (Costa et al., 2006), and satellites
78 (Alsdorf et al., 2007) may be considered. These instruments are safe and quick enough for
79 estimating river discharge. Fixed surface velocity, however, is difficult to measure since the
80 velocity of the water surface is normally affected by waves, winds and weather; thus, water
81 surface velocity is also problematic since studied areas and angles change in accordance
82 with water stages.

83 Measuring discharge levels using conventional methods and instruments during
84 flooding is frequently impossible and very impractical. Thus, many discharges are
85 determined after floods using indirect methods. Most indirect methods, such as the
86 slope-area method (Chow, 1973), step-backwater method (O'Connor and Webb, 1988),
87 contracted opening method (Benson and Dalrymple, 1967), and flow through culverts
88 (Bodhaine, 1968), assume a steady and uniform flow. Mountainous floods, which typically
89 move along steep river courses with debris, are generally unsteady and vary rapidly. Hence,
90 using indirect methods to calculate estimated discharges frequently results in significant
91 errors with accuracies rates of only 30% or greater (Bathurst, 1990). However, some
92 rediscovered techniques such as dilution gauging (McGuier et al., 2007) and rising bubble
93 method (Hilgersom and Luxemburg, 2012) can be used to measure discharge indirectly.

94 An accurate method and reliable equipment are needed to measure discharge from
95 mountain rivers during high flows. This study applies a novel method and flood discharge

96 measuring system that can be used to easily and accurately measure flood discharge of
97 mountain rivers in Taiwan. Section 2 is devoted to the measuring system which is composed
98 of an acoustic doppler current profiler, heavy sounding weight, wireless data transmission
99 system, and crane for measuring velocity profile quickly. I introduce my measurement
100 method for flood discharge that I refer to as “the efficient measurement method”. The
101 efficient method which makes use of maximum velocity and gauge height to estimate flood
102 discharge is developed in Section 3. In section 4, the flood discharge measured by the
103 proposed measurement system is used to illustrate the accuracy and reliability of the
104 measurement method.

105 **2. Flood discharge measuring system**

106 The flood discharge measuring system must withstand the worst possible weather
107 conditions and strong currents to observe and provide velocities and cross-sectional
108 information for discharge calculations. Instruments can be selected according to the
109 characteristics of each gauging station. Several different instruments are typically utilized to
110 collect data during high flows. The measurement of swift streams with highly unsteady flow
111 condition by current meter presents some problems such as impossible to sound and meter
112 drift downstream. Therefore it would be better not to submerge an instrument in the water
113 during high flow.

114 Based on Lu’s work (Lu et al., 2006), the Acoustic Doppler Profiler (ADP) is placed in

115 the C type sounding weight which is streamlined to offer minimum resistance to flow water.
116 The height of the sounding weight is less than 0.3 m. When the sounding weight is lowered to
117 the position under water surface 0.4 m, the sounding weight will be stationary in the water
118 and submerged sufficiently to avoid air entrainment beneath the transducer. The advantage of
119 the ADP is that it can immediately obtain velocity distribution and water-depth when ADP
120 touches water (Chen et al., 2007). When adequate sounding weights are used, the ADP can
121 stably measure velocity distribution in each of the selected verticals from water surface. The
122 key instrument of the flood discharge measuring system is the ADP which is a 3-axis water
123 current profiler. The resolution of velocity distribution and water depth depend on the
124 frequency of ADP. High frequency pings yield more precise data, but low frequency pings
125 travel farther in the water. So a compromise between the distance that the profiler can measure
126 and the precision of the measurements has to be made. Two ADPs with 3.0 and 1.5-MHz are
127 tested at the beginning of the flood discharge measurement. However the 1.5-MHz ADP
128 cannot be used near the right bank when water is too shallow. A 3.0-MHz ADP gives shorter
129 profiling ranges but better spatial resolution. The water depth of the Nanshih River at the
130 Lansheng Bridge is usually less than 6 m and the maximum profiling range of a 3.0-MHz
131 ADP is 6 m. Thus a 3.0-MHz ADP, which is suited to the hydrological characteristics of the
132 Nanshih River at the Lansheng Bridge, can collect velocity data.

133 The U.S. Geological Survey (USGS) has developed acoustic velocity meter systems for

134 river discharge observations since the mid-80s (Laenen, 1985) and using ADCPs on moving
135 boats for discharge measurements since the early 1990's (Oberg and Mueller, 1994), and
136 recently has it been used in observations (ISO, 2005). The profiling range of an ADP is
137 determined by its acoustic frequency. The performance of an ADP is also affected by
138 sediment concentration, air bubbles and the hydraulic situation in which it is placed. Hence,
139 an observer must first know the flow condition, concentration of suspended sediment, and
140 water depth to select the appropriate acoustic frequency. The ADP measures water velocity
141 using the Doppler shift, which is the shift of sound frequency reflected by a moving object
142 (Brumley et al., 1991). The ADP transmits sound at a fixed frequency and obtains echoes
143 returning from sound scatters in the water. These sound scatters are small particles, such as a
144 suspended load, that reflect sound back to the ADP (Boiten, 2003). The ADP transmits a short
145 pulse to measure relative water speed for many depth cells by range-gating the reflected
146 signal as a velocity distribution on a vertical. It also transmits a series of bottom-track pings
147 to determine water depth. Thus, during floods, an ADP can be placed on the water surface to
148 measure the velocity distribution and water depth on a vertical. Although velocity distribution
149 data can be obtained immediately, some areas were data is missing. Blanking distance is the
150 distance the emitted sound travels while internal electronics prepare for data reception and
151 the transducers stop vibrating from the transmission and become quiescent enough to
152 accurately record the backscattered acoustic energy (Mueller et al., 2007). Fig. 1 shows

153 transducer depth, blanking distance and bottom estimate, respectively. To obtain complete
154 data for the velocity distribution using the ADP, water depth cannot be less than 1.5 m. At
155 such depths, the current meter can be applied to measure the velocity distribution.

156 The suspended sounding weight is supported by the crane, the ADP is placed inside the
157 sounding weight, and the electronic assembly is placed inside a metal box located above the
158 sounding weight. The velocity distribution can be monitor on a laptop real time. The
159 electronics assembly supplies power for ADP and processes the signal sent from ADP. To
160 avoid damaging the flood discharge measurement system, application-specific carrying tools
161 and supports are required for the worst conditions. Thus, a 136 kg C type sounding weight
162 that is streamlined to offer minimum resistance to flowing water is used as the carrying
163 device for the ADP. This sounding weight stabilizes the ADP and avoids damage from being
164 struck by floating branches, junk and debris. The heavy weight of the sounding weight and
165 ADP makes it impossible to operate without the help of machinery. A mobile crane is used to
166 suspend the measuring system. This crane can be moved quickly among different locations.
167 Because strong currents can overturn sounding weights and destroy the cable between ADP
168 and the laptop, a wireless data transmission system is installed. The signals obtained by ADP
169 are first transmitted through a probe cable to an electronics assembly and then the data is then
170 sent to the radio telemetry system to transmit serial data to a wireless processing device - a
171 laptop. The velocity distribution and water depth can be measured instantaneously and then

172 calculated via data analyses. These data can be stored and saved on a computer for further
173 study.

174 Measurements are usually made from a bridge; the flood discharge measurement is best
175 carried out downstream of the bridge so the sounding weight does not collide with piers.
176 However the discharge measurement is made at upstream of the bridge. The reason of making
177 discharge at upstream of bridge is that the flow conditions are not affected by pier, less
178 bubbles are found to block signal, and is more stable. Additionally, the crane arm must be
179 long enough to suspend the sounding weight and position it far away from piers for avoiding
180 the sounding weight colliding piers.

181 **3. Computation of Flood Discharge**

182 The discharge equations for open channels are based on the velocity area method
183 (Herschy, 1999):

$$184 \quad Q = \bar{u}A \quad (1)$$

184 where Q is discharge; \bar{u} is mean velocity across a channel; and A is the cross-sectional area.

185 Flood discharge measurement of mountain rivers can be estimated directly using mean
186 velocity and cross-sectional area. The estimation of mean velocity is based on the relationship
187 between mean and maximum velocities, and the cross-sectional area can be estimated by
188 gauge height. Therefore estimating mean velocity of the cross-section from maximum
189 velocity is unique to the proposed method.

190 The relationship between mean and maximum velocities (Chiu, 1987) is

$$\frac{\bar{u}_{obs}}{u_{max}} = \phi \quad (2)$$

191 where u_{max} is the maximum velocity in a channel cross-section; $\bar{u}_{obs} = Q_{obs}/A_{obs}$; Q_{obs} is
 192 the observed discharge; and A_{obs} is the observed cross-sectional area. The ratio of \bar{u}_{obs} to
 193 u_{max} in a given cross-section, ϕ , approaches a constant (Chiu and Said, 1995; Chiu, 1996).
 194 It is a linear relationship passing through the origin. The ϕ ratio characterizes the flow
 195 pattern at a given channel cross-section, and can be applied to steady or unsteady flows and is
 196 unaffected by discharge or the water stage (Chen and Chiu, 2002). Different cross-sections of
 197 an open channel have different ratios (Chen and Chiu, 2004). Using ϕ ratio to estimate
 198 discharge of rivers has been implemented in several places including: Taiwan (Chen and Chiu
 199 2002), US (Chiu and Chen 2003), Italy (Moramarco et al. 2004), and Algeria (Ammari and
 200 Remini 2010). To determine flood discharge using Eq. (2), one must obtain many sets of \bar{u}
 201 and u_{max} to establish the relationship between maximum and mean velocities—the ϕ ratio.
 202 Once ϕ is determined, the flood discharge can be estimated quickly using maximum
 203 velocity and gauge height.

204 **3.1 Estimation of maximum velocity to determine ϕ**

205 To determine maximum velocity, an alternative velocity distribution model is needed
 206 that can describe the velocity distribution when maximum velocity is below the water surface.
 207 Chiu (1987) derived the following probabilistic velocity distribution equation:

$$\frac{u}{u_{\max}} = \frac{1}{M} \ln \left[1 + (e^M - 1) \frac{\xi - \xi_0}{\xi_{\max} - \xi_0} \right] \quad (3)$$

208 where ξ is the isovel in the $\xi-\eta$ coordinate system (Chiu and Chiou, 1988); u is velocity
 209 at ξ ; M is the entropy parameter; ξ_0 and ξ_{\max} are the maximum and minimum values of
 210 ξ at which $u = u_{\max}$ and $u=0$, respectively. y -axis is defined as the vertical on which u_{\max}
 211 occurs. One of the advantages of Eq. (3) is that it is capable of describing the velocity
 212 distribution whether maximum velocity occurs on or below water surface. Thus Eq. (3) can
 213 be used to determine the maximum velocity from the velocity distribution data measured by
 214 ADP, especially maximum velocity occurring under water surface. Since isovels are
 215 intercepted by the y -axis, where both ξ_{\max} and u_{\max} occur, the ξ values of the isovels can
 216 be expressed as a function of y on the y -axis

$$\xi = \frac{y}{D-h} \exp \left(1 - \frac{y}{D-h} \right) \quad (4)$$

217 where D is water depth on the y -axis; y is vertical distance from the channel bed; and h is the
 218 parameter indicating the location of u_{\max} . If u_{\max} occurs on the water surface, $h \leq 0$, and
 219 Eq. (3) becomes

$$\frac{u}{u_{\max}} = \frac{1}{M} \ln \left[1 + (e^M - 1) \frac{y}{D} \exp \left(\frac{D-y}{D-h} \right) \right] \quad (5)$$

220 If u_{\max} occurs below the water surface, $h > 0$ and h is the actual depth of u_{\max} below the
 221 water surface, and Eq. (3) becomes

$$\frac{u}{u_{\max}} = \frac{1}{M} \ln \left[1 + (e^M - 1) \frac{y}{D-h} \exp \left(1 - \frac{y}{D-h} \right) \right] \quad (6)$$

222 Although the location of u_{\max} in an open-channel is not determined easily, it can be
 223 obtained using the isovels created with velocity data collected previously. In natural rivers,
 224 the y-axis can occur anywhere around the cross-section. If the cross-section of a relatively
 225 straight open channel does not change drastically, the location of y-axis is extremely steady
 226 and does not vary according to changes in time, water level, and discharge (Chiu and Chen,
 227 2003). Restated, the likely location of the y-axis can be identified using historical data, and
 228 the maximum velocity of a cross-section can be obtained using the y-axis. Statistically, one
 229 standard deviation of distance from the y-axis can be used to identify the stability of the
 230 y-axis (Chiu and Chen, 1999). The maximum velocity obtained by data from around the
 231 y-axis and the actual value are very close; thus, a slight shift in the y-axis will not cause
 232 significant error in the estimated maximum velocity (Chiu and Chen, 2003). However ADP
 233 cannot sample the velocity near water surface and the velocity distribution is not continue.
 234 Hence, the nonlinear regression model can be fitted to velocity distribution data on the y-axis
 235 measured by the ADP to Eq. (3) for determining maximum velocity in the cross-section.

236 3.2 Estimation of mean velocity to determine ϕ

237 The mean velocity of the channel used to establish the relationship between mean and
 238 maximum velocities is determined by Q_{obs}/A_{obs} . Thus, measuring flood discharge using the

239 conventional method becomes a very important but difficult task. The conventional method
 240 divides the cross-section into segments by spacing verticals at an appropriate number of
 241 locations across the channel. USGS suggests using 6 to 10 observation verticals in the
 242 measurement cross section for a small stream. Reduce the number of sections taken to about
 243 15-18 during periods of rapidly changing stage on large streams (Rantz, 1982). Distance
 244 between verticals, depth, and velocities are measured at the verticals. A sounding weight or
 245 ADP is utilized to measure water depths at the verticals. The velocities at the verticals are
 246 measured using a current meter or ADP. Segment discharges are computed between
 247 successive verticals; therefore, total discharge may be computed as

$$Q_{obs} = \sum q_i \quad (7)$$

$$q_i = \bar{v}_i a_i \quad (8)$$

248 where q_i is the i^{th} segment discharge; \bar{v}_i is the individual segment mean velocity normal to
 249 the segment; and a_i is the corresponding area of the segment. Notably, a_i can be
 250 determined using the midsection method.

251 **3.3 Estimation of cross-sectional area**

252 The cross-sectional area and gauge height data are collected during discharge
 253 measurement. The segment areas are summed to obtain the cross-sectional area of the open
 254 channel. If the streambed is stable and free of scouring and deposits, it is normally reliable to
 255 estimate cross-sectional area with gauge height. The relationship between cross-sectional area

256 and gauge height (Chen and Chiu, 2002) can be expressed as

$$A_{est} = a(G - b)^c \quad (9)$$

257 where A_{est} is the estimated cross-sectional area; G is gauge height. a , b , and c are
 258 coefficients determined by nonlinear regression. Compared to the cross-sectional area during
 259 flood, when the area caused by scouring or depositing is small. Eq. (10) can also be applied to
 260 estimate cross-sectional area. If the relation of G and A_{obs} is not good enough, it could be a
 261 large source of uncertainty in the final discharge.

262 **3.4 Estimation of the discharge by the efficient measurement method**

263 Before the discharge estimation method, referred to as the efficient measurement method,
 264 is developed in a stream, obtaining \bar{u}_{obs} to determine ϕ for a given cross-section in a
 265 stream is the key in developing the efficient method. The observed mean velocity of the
 266 cross-section is calculated as Q_{obs}/A_{obs} . The complete flood discharge measurements over
 267 the full cross-section are very important for establishing the relationship between mean and
 268 maximum velocities and it possibly will take several years to collect enough data. Therefore
 269 it is necessary to measure discharge and cross-sectional area by sampling velocities and depth
 270 in each vertical for determining mean velocity in each vertical and segment area. Then the
 271 discharge is derived from the sum of the product of mean velocity, depth and width between
 272 verticals. The velocity distribution made on y-axis is used to calculate maximum velocity of
 273 the cross-section for determining ϕ . The gauge height and cross-sectional area are used to

274 establish the relation of gauge height and cross-sectional area.

275 Looking for the location of y-axis in a stream is difficult. For a straight and regular
276 artificial channel, the y-axis usually occurs at the center of the cross-section. The location of
277 y-axis in a natural channel can be located anywhere in the cross-section. Fortunately, the
278 velocities used to determine the discharge reveal the location of y-axis. By using the
279 measured velocity data, isovel patterns of a stream can indicate the location of y-axis.

280 Once the efficient method is established, only the velocity distribution on y-axis and
281 gauge height are needed to be measured for estimating flood discharge. The maximum
282 velocity determined by velocity distribution and ϕ can be used to estimate mean velocity of
283 the cross-section. The cross-sectional area can be determined by the gauge height. Finally the
284 flood discharge can be easily be estimated by $\phi u_{\max} A_{est}$.

285 4. Description of study catchment and data

286 The study site is located at the Lansheng Bridge on the Nanshih River. Fig. 2 shows the
287 locations of the catchment area and gauge stations. Situated southeast of Taipei, Taiwan, the
288 Nanshih River, an upstream branch of the Tanshui River, is a major fresh water source for the
289 Taipei metropolitan area. To safeguard water quality and quantity, access to this area is
290 restricted; thus, most of the area is untouched and forested. The area covers 331.6 km² and
291 has an annual precipitation of 3082–4308 mm (average, 3600 mm). Days with precipitation
292 are mostly concentrated in winter. The northeastern winds in winter create fine rain, whereas

293 typhoons in summer bring heavy rains. The average monthly precipitation in the area from
294 June to October exceeds 300 mm from 1992. Although a discharge measuring system that is
295 composed of radar sensor for measuring water stage and current meter for measuring velocity
296 has been in place on the Lansheng Bridge since 2005, flood discharge was not measured until
297 2007. The average discharge of the Nanshih River at the Lansheng Bridge is 26.9 m³/s; the
298 minimum is 0.9 m³/s, and the maximum is 2295 m³/s. The Nanshih River is about 35 km long
299 to the Lansheng Bridge and 45 km to the confluence of the Nanshih River and the Beishih
300 River; the highest altitude is 2,101 m on Mount Babobkoozoo, and the altitude of the river
301 bed at the Lansheng Bridge is 106.8 m. Thus the stream gradient, which is the grade
302 measured by the ratio of drop in elevation of a stream per unit horizontal distance, of the
303 upstream of the Nanshih River exceeds 10% and the average stream gradient to the
304 Lansheng Bridge is 5.7%. The stream gradient at the study site is about 1.5%, which is still
305 relatively steep.

306 **5. Measurement of Flood Discharge**

307 This study was conducted on the Nanshih River at the Lansheng Bridge from 2007 to
308 2010. During the typhoon season, flood discharges were measured using the proposed flood
309 measurement system. Fig. 3 shows the flood discharge measurement during Typhoon Krosa.
310 Since maximum water depth during the non-typhoon season is usually less than 1.5 m,
311 discharge is measured by current meter, not the ADP. At the y-axis (22 m from relative point

312 situated at the left bank), velocity measurements are taken at 0.1 m intervals from the water
313 surface to the channel bed when water is shallow and the ADP cannot be applied to measure
314 velocity distribution.

315 The velocity distribution and water depth are measured at 3 m intervals during the
316 typhoons for computation of discharge. The probabilistic velocity distribution equation is
317 then utilized to simulate velocity profiles and calculate the mean velocities of the verticals.
318 Finally, each segmental discharge can be obtained, the sum of which is the river discharge. As
319 shown in Fig. 4, the flood discharge per unit width, mean velocity at each vertical and the
320 corresponding depth are plotted over the water surface line. The top of Fig. 4 is the segmental
321 mean velocity and discharge, and the bottom is the flow pattern. It also shows that most of
322 discharge occurs in the main channel. By using the ADP, the cross-section can be easily and
323 quickly surveyed for determining cross-sectional area. Table 1 shows the ADP measurements
324 taken during typhoons in 2007 and 2008, of which 8 discharges were measured for five
325 typhoons.

326 The bottom of Fig. 4 shows the velocity distribution of maximum measured flood
327 discharge in 2007. z in Fig. 4 is the distance from relative point. The discharge was around
328 185.3 m^3/s . The dot in Fig. 4 is the actual velocity measurement on each vertical, and the
329 solid line is the velocity distributions based on Eq. (3), indicating that vertical maximum
330 velocity does not always occur on the water surface. Additionally, no definite relationship

331 exists between mean and water surface velocity of the river. Hence, an accurate measurement
332 of flood discharge must be based on the flow pattern below the water surface and not water
333 surface velocity. However, if the maximum velocity always occurs on water surface, the
334 relationship between mean and surface velocity can be developed using Eq. (2). The
335 maximum velocity occurred at the vertical, 22 m away from the relative point. The maximum
336 velocity of the cross-section estimated by Eq. (3) was 4.83 m/s and occurred on the water
337 surface. Fig. 5 shows the isovels based on the observed velocities in Fig. 4. In Fig. 5, the
338 vertical dash line reveals the location of y-axis. Owing to the effect of bridge piers, velocities
339 around $z = 15$ m and $z = 37$ m are lower. Both Figs. 4 and 5 indicate that the major flood
340 discharges are 15–30 m from the relative point, a sign that velocity on the right bank is slow,
341 and the maximum velocity occurs around the 6th vertical from the left bank and on the water
342 surface. Additionally, the observations of other flow patterns indicate that the maximum
343 velocities always occur on the 6th vertical. This finding suggests that the y-axis locates on the
344 6th vertical. The y-axis is stable and unaffected by other factors such as stages and discharges.
345 Fig. 6 shows the cross-sectional variation of the channel bed. The main course of the river
346 bed does not change drastically, whereas the right side of the river bed has obvious scouring
347 and deposition during flooding. For instance, on 28 November, the right bank shows obvious
348 signs of scouring, and on 29 November, is deposited; the cross-section gradually returns to its
349 previous stage. Based on the cross-section on 29 November, the scouring and depositing

350 areas in the cross-section on 8 October and 28 November are 13.9 and 7.74 m², respectively.

351 Table 2 shows the variation of area between two typhoon events. The area varies slightly

352 between Typhoon and Krosa. At the beginning of Typhoon Mitag, the right side of the river

353 bed is scoured deeply. However the Nanshih River tends to deposit its sediment in the end of

354 Typhoon Mitag. After scouring and depositing, the change in area is 6.7 m² between Typhoon

355 Sepat and Typhoon Sinlaku. It shows that the Nanshih River at the Lansheng Bridge is in the

356 conditions of dynamic stability and near-equilibrium. Comparing with the cross-sectional

357 area during flood, the scouring and depositing areas are relatively small. Therefore the

358 observed cross-sectional areas can be used to establish the relation of water stage and

359 cross-sectional area.

360 The data of discharge is split into two independent subsets: the calibration and validation

361 subsets. The calibration subset with 19 observed discharges is used for parameter estimation.

362 The validation subset, which consists of 5 observed discharges, is devoted to assess the

363 performance of the proposed method. Correlation coefficient indicating the strength of

364 relationship between observed and estimated discharges and root-mean-square error (RMSE)

365 evaluating the residual of observed and estimated discharges are used to evaluate the

366 performance of the efficient method.

367 An efficient method of measuring flood discharges of mountain rivers can be established

368 through repeated measurements. Fig. 7 shows the relationship between mean and maximum

369 velocities of the Nanshih River at the Lansheng Bridge. It is a straight line goes through
370 origin, and $\bar{u}_{est} = 0.51u_{max}$. The maximum velocity of the cross-section can be calculated by
371 Eq. (4), and the mean velocity is obtained by dividing the measured discharge by the
372 cross-sectional area. All maximum velocities during floods exceed 3 m/s, whereas the u_{max}
373 on ordinary days can reach 0.8 m/s, indicating a swift current. Moreover, the relationship
374 between mean and maximum velocities is constant and quite stable in a wide range of
375 discharge. It does not vary with time, water stage and sediment concentration, regardless of
376 whether the flow is steady or unsteady. Using gauge height and cross-sectional area, the
377 relationship between stage and area can be established. It is $A_{est} = 14.39(G - 107.32)^{1.68}$, as
378 shown in Fig. 8. Fig. 9 shows the accuracy of the cross-sectional area estimated by the water
379 stage. The correlation coefficients in both phases of calibration and validation are very high
380 and RMSEs are low. The estimated areas agree quite well with the observed areas. Therefore,
381 during floods, cross-sectional areas can be estimated based on gauge height.

382 During flood, maximum velocity can be observed on the y-axis, 22 m from the relative
383 point. The channel cross-sectional area is calculated using gauge height, and mean velocity is
384 obtained using the ϕ value and maximum velocity. Finally, discharge can be estimated by
385 $Q_{est} = 7.34u_{max}(G - 107.32)^{1.68}$. Fig. 10 shows the evaluation of discharge estimation accuracy
386 for the Nanshih River at the Lansheng Bridge. All the data points nicely fall on the line of
387 agreement. The RMSE of the calibration and evaluation are 16.4 and 15.2 m³/sec. Moreover,

388 the ρ of the calibration and evaluation are 0.99 and 0.96, respectively. The results show that
389 the method performance is accurate and consistent in two different subsets. Both correlation
390 coefficients are very close to unity, and both RMSEs are relatively smaller. It demonstrates
391 that the proposed method can be successfully applied to estimate flood discharge of mountain
392 rivers.

393 Fig. 11 shows the frequency functions for a normal distribution fitted to the ε %. Fig.
394 11(a) shows the relative frequency of error percentage. Fig. 11(b) shows the cumulative
395 frequency (dots) and probability distribution function (curve). The mean of the errors
396 approaches zero and the absolute measure of error is 7%. Thus the 95.44% confidence
397 interval for the discharge error is from -2.11% to 2.69%. The χ^2 test is employed to determine
398 whether the normal distribution adequately fits data. The χ^2 test statistic is $\chi_c^2=0.57$ and the
399 value of $\chi_{\nu,1-\alpha}^2$ for a cumulative probability is $\chi_{2,0.95}^2=5.99$. Since $\chi_{2,0.95}^2 > \chi_c^2$, these errors
400 are mutually independent and normally distributed with a mean approaching zero and small
401 variance. Clearly, the proposed method can be utilized to accurately and reliably measure
402 flood discharge of mountain rivers.

403 The gauge station on the Lansheng Bridge was established in 2005 and it collected
404 discharge data under low water levels by using the current meter method. In 2007, the station
405 began to be used to collect data under high water levels with the method developed in this
406 paper. Once the efficient method for measuring flood discharge of mountain rivers is

407 established, the flood discharges during Typhoon Jangmi in 2008 are estimated only
408 depending on maximum velocities and gauge heights. Fig. 12 shows the velocity distribution
409 measured by ADP on y -axis during Typhoon Jangmi. Therefore the maximum velocity can be
410 calculated by using Eq. (3) with the collected velocity distribution. The estimated flood
411 discharges during Typhoon Jangmi are summarized in Table 3. In Table 3, Q is discharge
412 estimated by the proposed method, and Q_r is discharge estimated by stage-discharge rating
413 curve. The discharge estimated by only the velocity distribution on y -axis is very close to the
414 discharge estimated by rating curve. It shows that the method presented in this paper is
415 reliable and accurate for estimating flood discharge. By using the proposed method, the flood
416 discharge can be estimated quickly within 1 minute.

417 Real-time discharge at a stream-gauging station can be computed from a real-time stage
418 using the stage-discharge relationship, which is also called the rating curve. Recorded
419 discharges over a wide range are rare. Notably, measurement accuracy of conventional
420 instruments and methods can be adversely affected and restricted by both location and
421 weather; these instruments are most reliable during stable and low-flow conditions. Thus,
422 long-term observations can be used to establish the lower part of a rating curve. However, to
423 create a complete rating curve, high flow discharge data are needed. Fig. 13 is the water-stage
424 rating curve of the Nanshih River at the Lansheng Bridge. When water stages are 113, 112,
425 and 111 m, the differences between the discharges estimated by the old and new rating curve

426 are 118, 109, and 81 m³/s, respectively. The old rating curve severely underestimates
427 discharge under high water levels, whereas the curve for 2010 was likely adjusted according
428 to flood discharge, markedly improving its accuracy and efficiency. It indicates that the
429 importance of flood discharge for establishing a stage-discharge rating curve. The accurate
430 rating curve with the actual measurements during high water also demonstrates this method
431 has improved the overall discharge measurement of the river.

432 **6. Conclusions**

433 Flood discharge measurement is always a difficult and dangerous task. The
434 characteristics of mountain rivers make it impractical to use conventional methods and
435 instruments to measure discharges during floods. Concerns for personal safety, accuracy,
436 reliability, and efficiency, a new measurement method and system have to be developed for
437 flood discharge measurement in Taiwan. According to the hydrological characteristics of the
438 Nanshih River at the Lansheng Bridge, a flood measuring system composed of useful
439 techniques and tools is applied to collect velocity and water depth data over the full
440 cross-section for calculating discharge and determining the location of y-axis. The efficient
441 discharge measurement method based on the relation of mean and maximum velocities and
442 the relation of gauge height and cross-sectional area is developed to estimate the flood
443 discharge in the Nanshih River at the Lansheng Bridge. Therefore the flood discharge can be
444 easily estimate by sampling gauge height and the velocity distribution on y-axis for

445 calculating maximum velocity. Those flood data used for establishing stage-discharge rating
446 curve makes real time flood discharge estimation possible. Like the other index velocity
447 methods converting the velocity at a point or in a section to the mean velocity, the efficient
448 method is also an index velocity method for measuring flood discharge in mountain rivers.
449 The merits of the proposed measuring system and method for measuring flood discharge of
450 mountain rivers in Taiwan are as follows: 1) considerably accuracy and efficiency; 2) flood
451 discharges can be measured - an impossible task previously; and, 3) hydrologists are not
452 exposed to harsh environments during typhoons and floods too long. The proposed
453 measurement system is used to measure flood discharge in the mountain area of Taiwan to
454 verify this efficient method. The results provide evidence that this efficient method can offer
455 good performance in measuring flood discharge of the Nanshih River at the Lansheng
456 Bridge.

457 This research is limited to an initial study of the application of the efficient method in
458 estimating flood discharge in the Nanshih River at the Lansheng Bridge. Further studies
459 could be extended to measure more flood discharges of the other mountain rivers for
460 validating the efficient method. Even the proposed method is a fast and minimally intrusive
461 measurement method; it is still very dangerous to measure the velocity distribution on y-axis
462 during floods. It is necessary to develop a model for estimating maximum velocity not on
463 y-axis.

464 **Acknowledgements**

465 The author is indebted to anonymous reviewers for their valuable comments and
466 suggestions. The author would like to thank the Taipei Water Management Office, Water
467 Resources Agency of Taiwan, for financially supporting this research. Contributions by Profs.
468 J.-T. Kuo and H.-C. Yang are also gratefully acknowledged.

469 **References**

- 470 Alsdorf, D. E., Rodriguez, T., and Lettenmaier, D. P.: Measuring surface water from space,
471 Rev. Geophys., 45, 1-24, 2007.
- 472 Ammari, A. and Remini, B.: Estimation of Algerian rivers discharges based on Chiu's
473 equation, Arab. J. Geosci., 3, 59-65, 2010.
- 474 Bandyopadhyay, J., Rodda, C. J., Kattelmann, R., Kundzewicz, Z. W., and Kraemer, D.:
475 Highland waters – a resource of global significance, in: Mountains of the World: A
476 Global Priority, Parthenon, London, UK, 131-155, 1997.
- 477 Bathurst, J. C.: Tests of three discharge gauging techniques in mountain rivers, In: Hydrology
478 of Mountainous Areas, IAHS, Wallingford, UK, 93-100, 1990.
- 479 Benson, M. A. and Dalrymple, T.: General field and office procedures for indirect discharge
480 measurement, US Governmental Printing Office, Washington DC, Techniques of
481 Water-Resources Investigations, Book 3, 30 pp., 1967.
- 482 Bodhaine, G. L.: Measurement of peak discharge at Culverts by indirect methods, US

- 483 Governmental Printing Office, Washington DC, Techniques of Water-Resources
484 Investigations, Book 3, 19pp., 1968.
- 485 Boiten, W.: Hydrometry, A.A. Balkema, Lisse, The Netherlands, 2003.
- 486 Brumley, B. H., Cabrea, R. G., Deines, K. L., and Terray, E. A.: Performance of a broad-band
487 acoustic Doppler current profiler, IEEE J. Oceanic Eng., 16, 402-407, 1991.
- 488 Bureau of Reclamation: Water measurement manual, US Government Printing Office,
489 Denver, 1997.
- 490 Chen, Y.-C. and Chiu, C.-L.: A fast method of flood discharge estimation, Hydrol. Process.,
491 18, 1671-1684, 2004.
- 492 Chen, Y.-C. and Chiu, C.-L.: An efficient method of discharge measurement in tidal streams,
493 J. Hydrol., 265, 212-224, 2002.
- 494 Chen, Y.-C., Kuo, J.-T., Yang, H.-C., Yu, S.-R., and Yang, H.-Z.: Discharge measurement
495 during high flow. J. Taiwan Water Conserv., 55, 21-33, 2007. (in Chinese)
- 496 Chiu, C.-L.: A natural law of open-channel flows, In: Stochastic Hydraulics '96, Balkema,
497 Rotterdam, The Netherlands, 15-27, 1996.
- 498 Chiu, C.-L.: Entropy and probability concepts in hydraulics, J. Hydraul. Eng.-ASCE, 113,
499 583-600, 1987.
- 500 Chiu, C.-L. and Chen, Y.-C.: Efficient methods of measuring discharge and reservoir-sediment
501 flow, In: Risk analysis in dam safety assessment, Water Resources Publications, LLC,
502 Highlands Rauch, Colorado, 1999.

- 503 Chiu, C.-L. and Chen, Y.-C.: An efficient method of discharge estimation based on
504 probability concept, *J. Hydraul. Res.*, 41, 589-596, 2003.
- 505 Chiu, C.-L. and Chiou, J.-D.: Entropy and 2-D velocity distribution in open channels, *J.*
506 *Hydraul. Eng.-ASCE*, 114, 738-756, 1988.
- 507 Chiu, C.-L. and Said, C. A. : Maximum and mean velocities and entropy in open-channel
508 flow, *J. Hydraul. Eng.-ASCE*, 121, 26-35, 1995.
- 509 Chow, V. T.: *Open-Channel Hydraulics*, McGraw-Hill, Singapore, 1973.
- 510 Costa, J. E., Cheng, R. T., Haeni, F. P., Melcher, N., Spicer, K. P., Hayes, E., Plant, W., Hayes,
511 K., Teague, C., and Barrick, D.: Use of radars to monitor stream discharge by noncontact
512 methods, *Water Resour. Res.*, 42, W07422, doi:10.1029/2005 WR004430, 2006.
- 513 Herschy, R. W.: *Hydrometry*, Wiley, West Sussex, England, 1999.
- 514 Hilgerso, K. P. and Luxemburg, W. M. J.: Technical Note: How image processing facilitates
515 the rising bubble technique for discharge measurement, *Hydrol. Earth Syst. Sci.*, 16,
516 345-356, 2012.
- 517 International Organization for Standardization (ISO): *Hydrometry–Measuring river velocity*
518 *and discharge with acoustic Doppler profilers*, ISO, Geneva, Ref. No. ISO 24154, 2005.
- 519 International Organization for Standardization (ISO): *Hydrometry–Measurement of liquid*
520 *flow in open channels using current-meters or floats*, ISO, Geneva, Ref. No. ISO 748,
521 2007.

- 522 Jarrett, R. D.: Hydraulics of mountain rivers, In: Channel Flow Resistance: Centennial of
523 Manning's Formula, Water Resources Publications, Littleton, Colorado, 287–298 ,1992.
- 524 Laenen, A.: Acoustic velocity meter systems, US Governmental Printing Office, Washington
525 DC, Techniques of Water-Resources Investigations, 1985.
- 526 Le Coz, J., Pierrefeu, G., and Paquier, A.: Evaluation of river discharges monitored by a fixed
527 side-looking Doppler profiler, Water Resour. Res., 44, W00D09,
528 doi:10.1029/2008WR006967, 2008.
- 529 Lu, J.-Y., Su, C.-C., and Wang, C.-Y.: Application of a portable measuring system with
530 acoustic Doppler current profiler to discharge observations in steep rivers, Flow Meas.
531 Instrum., 17, 179-192, 2006.
- 532 McGuire, K. J., Weiler, M., and McDonnell, J. J.: Integrating tracer experiments with
533 modeling to assess runoff processes and water transit times, Adv. Water Resour., 30,
534 824-837, 2007.
- 535 Moramarco, T., Saltalippi, C., and Singh, V. P.: Estimation of mean velocity in natural
536 channels based on Chiu's velocity distribution equation, J. Hydraul. Eng.-ASCE, 9, 42-50,
537 2004.
- 538 Mueller, D. S., Abad, J. D., Garcia, C. M., Gartner, J. W., Gracia, M. H., and Oberg, K. A.:
539 Errors in acoustic Doppler profiler velocity measurements caused by flow disturbance, J.
540 Hydraul. Eng.-ASCE, 133, 1411-1420, 2007.

- 541 Nihei, Y. and Kimizu, A.: A new monitoring system for river discharge with horizontal
542 acoustic Doppler current profiler measurements and river flow simulation, *Water Resour.*
543 *Res.*, 44, W00D20, doi:10.1029/2008WR006970, 2008.
- 544 Oberg, K. A. and Mueller, D. S.: Recent applications of acoustic Doppler current profilers, In:
545 *Proceedings of the Symposium on Fundamentals and Advancements in Hydraulic*
546 *Measurements*, Buffalo, New York, 1-5 August 1994, 341-350, 1994.
- 547 O'Connor, J. E., and Webb, R. H.: Hydraulic modeling for paleoflood analysis, In: *Flood*
548 *Geomorphology*, Wiley, New York, 393-402, 1988.
- 549 Rantz, S. E.: *Measurement and Computation of Streamflow: Volume 1. Measurement of*
550 *Stage and Discharge*, US Governmental Printing Office, Washington DC, Water-Supply
551 *Paper 2175*, 1982.
- 552 Viviroli, D. and Weingartner, R.: The hydrological significance of mountains: from regional
553 to global scale, *Hydrol. Earth Syst. Sci.*, 8, 1016-1029, 2004.
- 554 WMO: *WMO technical regulations: Volume III. Hydrology*, World Meteorological Organization,
555 Geneva, No. 49, 1988.

Table 1. Flood discharge measurement of the Nansih River by using ADP at the Lansheng

Bridge in 2007 and 2008.

Typhoon	Date	G (m)	A_{obs} (m ²)	Q_{obs} (m ³ /s)
Sepat	9/8/2007	110.95	142.5	308.6
		110.77	119.0	266.2
Wipha	9/19/2007	110.31	91.7	171.9
Krosa	10/7/2007	111.57	169.2	447.6
	10/8/2007	110.50	101.3	185.3
Mitag	11/28/2007	110.45	118.8	193.6
	11/29/2007	109.88	86.6	136.8
Sinlaku	9/15/2008	111.52	146.9	341.1

Table 2. Area variation between two typhoon events.

Typhoon	Date	G (m)	A_v (m ²)	%
Sepat	9/8/2007	100.95		
		110.77	4.1	2.9
Wipha	9/19/2007	110.31	-3.4	-2.9
Krosa	10/7/2007	111.57	-5.3	-5.8
	10/8/2007	111.50	-0.1	-0.1
Mitag	11/28/2007	111.45	-22.5	-22.2
	11/29/2007	109.88	6.7	5.6
Sinlaku	9/15/2008	111.52	27.0	31.2
Total			6.7	

Table 3. Flood discharge of the Nanshih River at the Lansheng Bridge estimated by the efficient method during Typhoon Jangmi in September 28, 2008.

Time	G (m)	u_{\max} (m/s)	\bar{u}_{est} (m/s)	A_{est} (m ²)	Q_{est} (m ³ /s)	Q_r (m ³ /s)	$Q_{est}-Q_r$ (m ³ /s)
11:35 am	112.30	4.05	2.09	213.8	448.6	496.3	-47.7
12:35 pm	112.20	4.51	2.33	207.8	485.4	475.9	9.5
2:05 pm	112.30	4.43	2.29	213.9	504.6	496.3	8.3
2:54 pm	112.63	4.22	2.18	233.9	511.3	566.4	-55.1
3:58 pm	113.18	4.93	2.55	268.0	684.4	691.6	-7.2

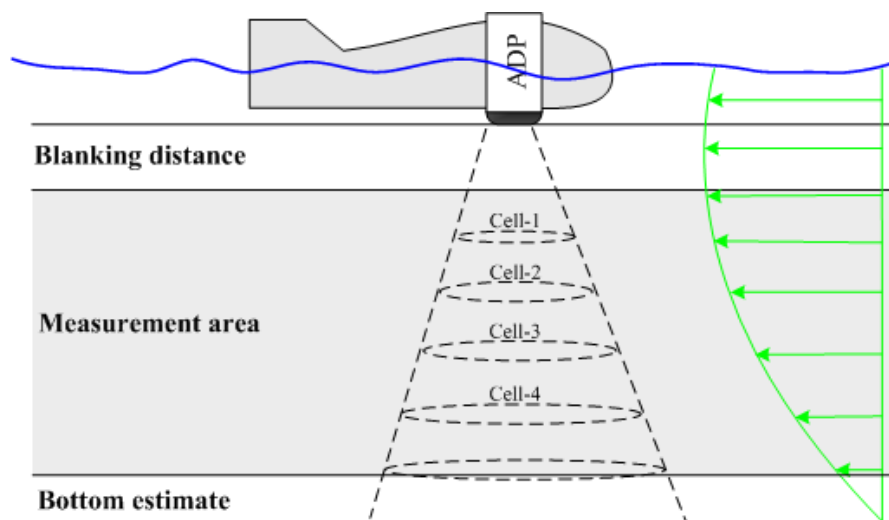


Fig. 1. Unmeasured areas of ADP.

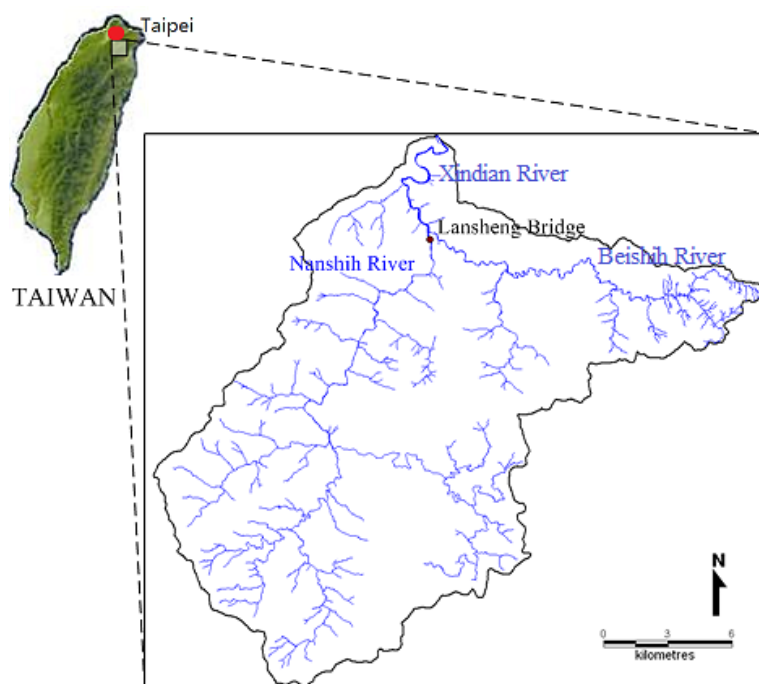


Fig. 2. Location of the study site in the catchment of the Nanshih River, Taiwan.



Fig. 3. Flood discharge measurement during Typhoon Krosa.

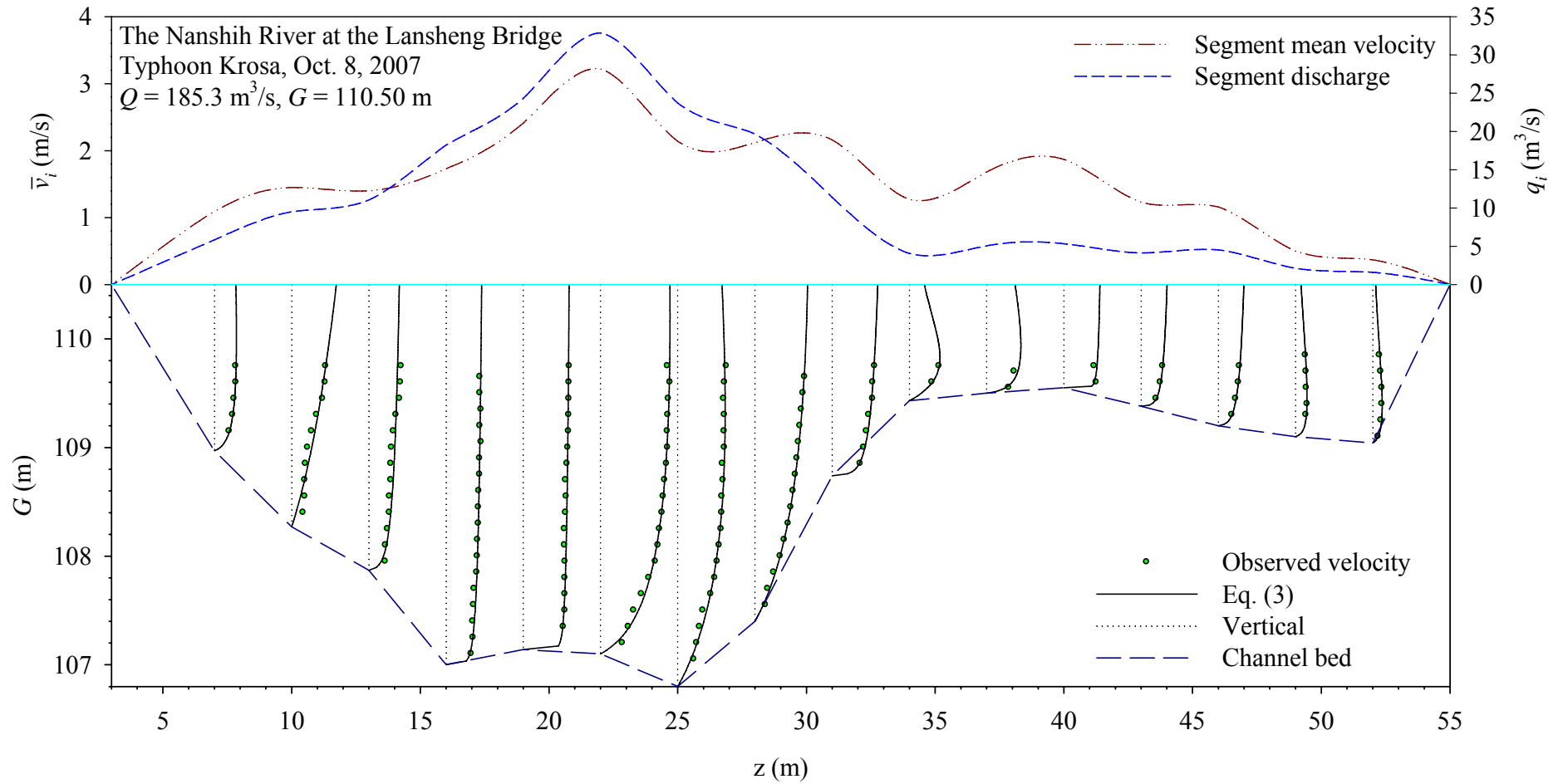


Fig. 4. Depth velocity graph during Typhoon Krosa (Oct. 8, 2007).

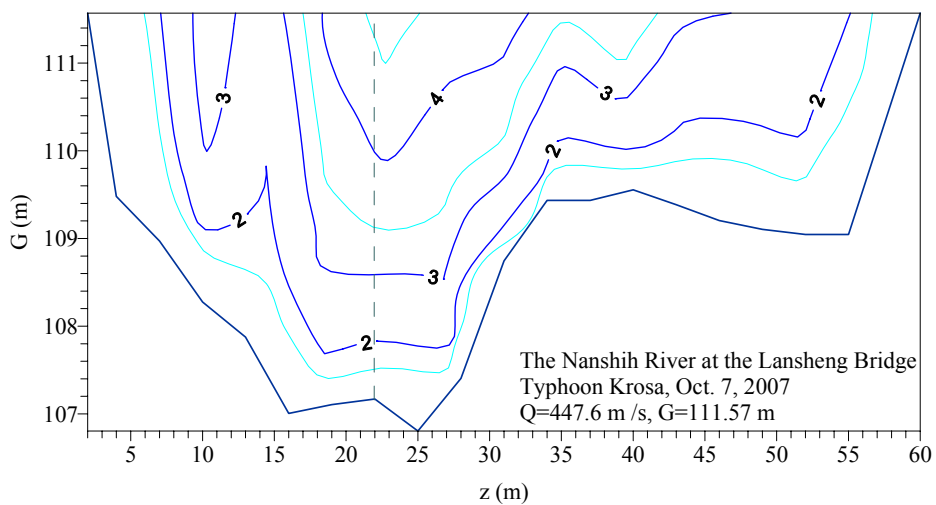


Fig. 5. Isovels in the Nanshih River at the Lansheng Bridge during Typhoon Krosa.

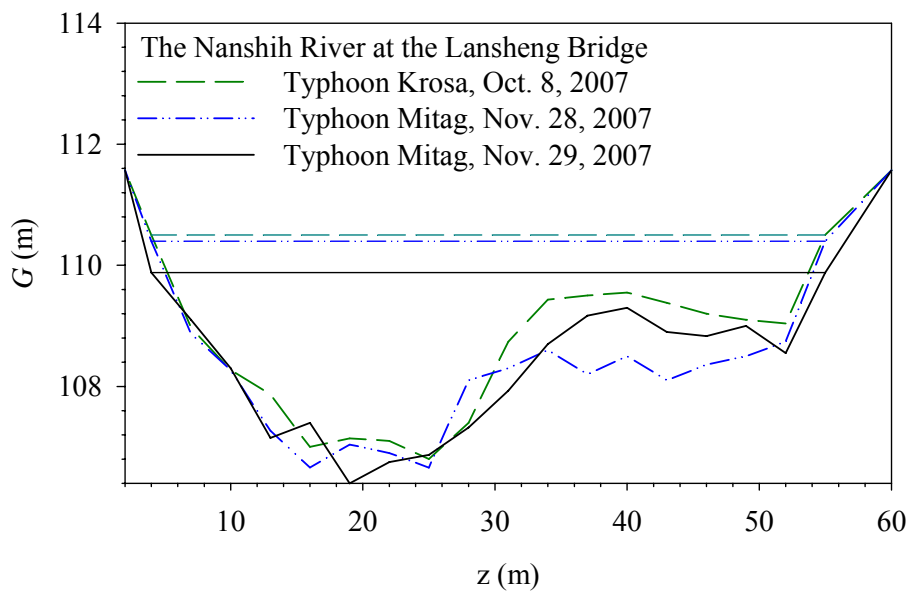


Fig. 6. Scour and deposit of channel bed during Typhoon Mitag.

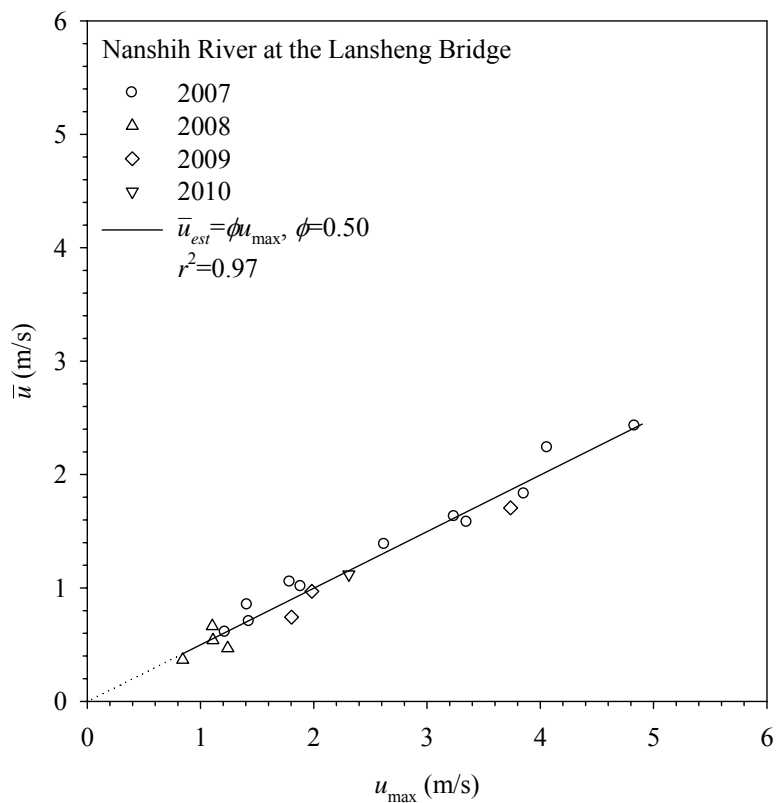


Fig. 7. Relation between mean and maximum velocities.

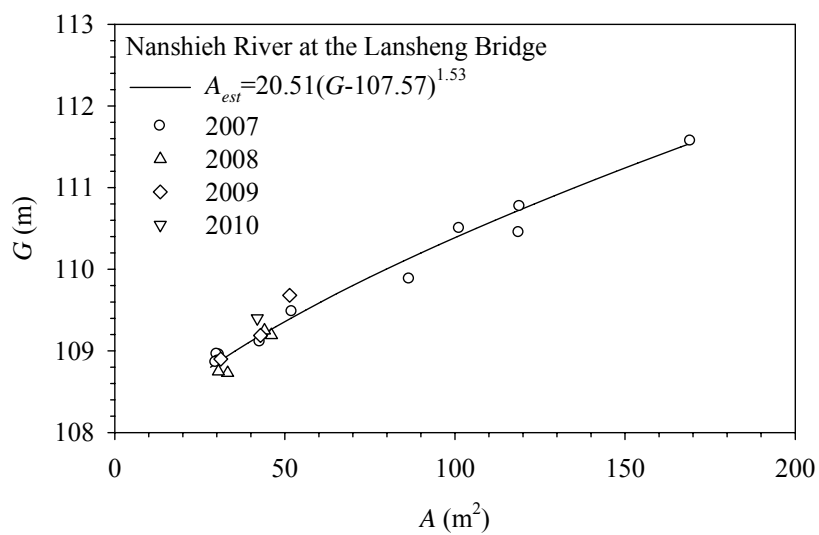
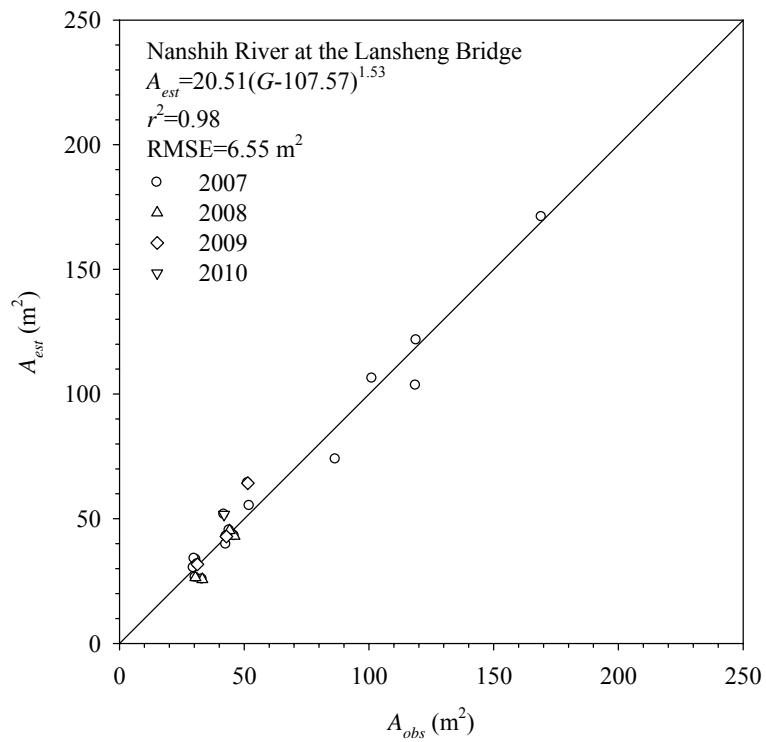
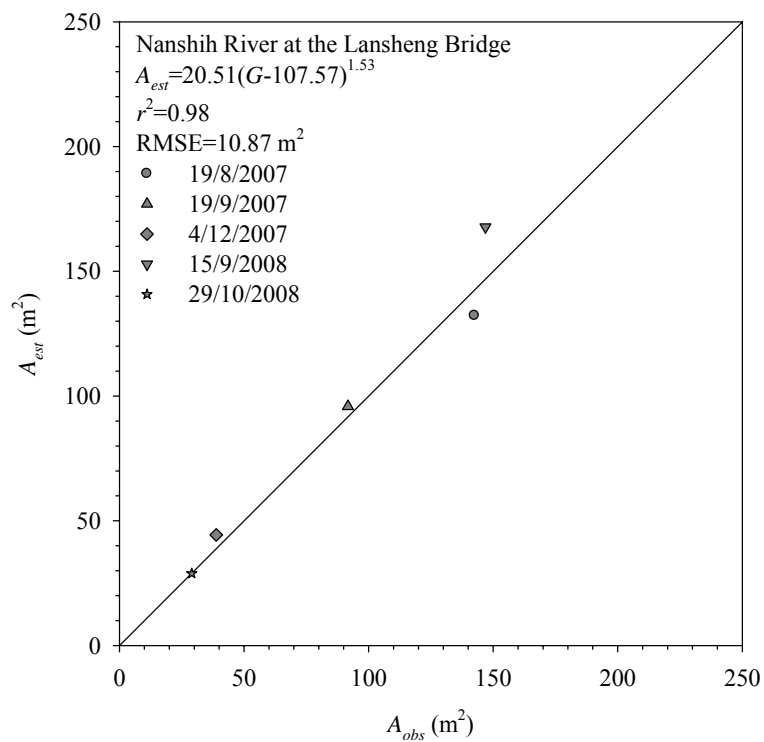


Fig. 8. Relation between gauge height and cross-sectional area.

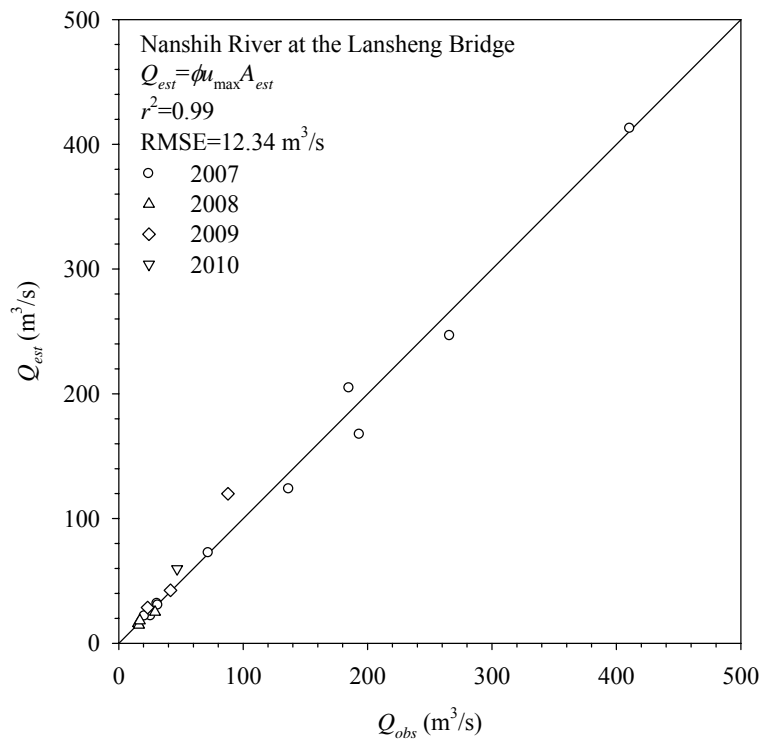


(a)

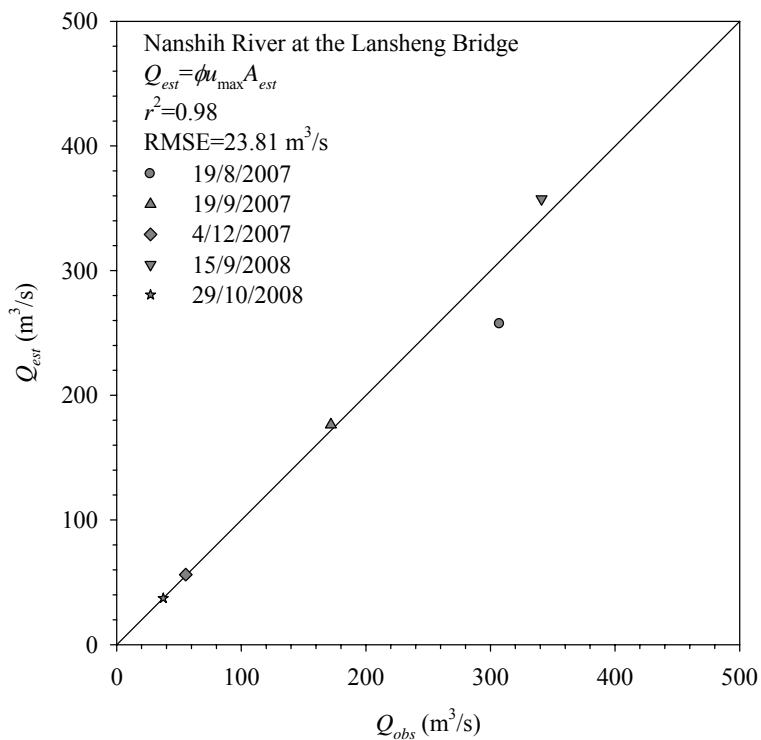


(b)

Fig. 9. Accuracy of estimated cross-sectional area in the Nanshih River at the Lansheng Bridge; (a) Calibration; (b) Validation.

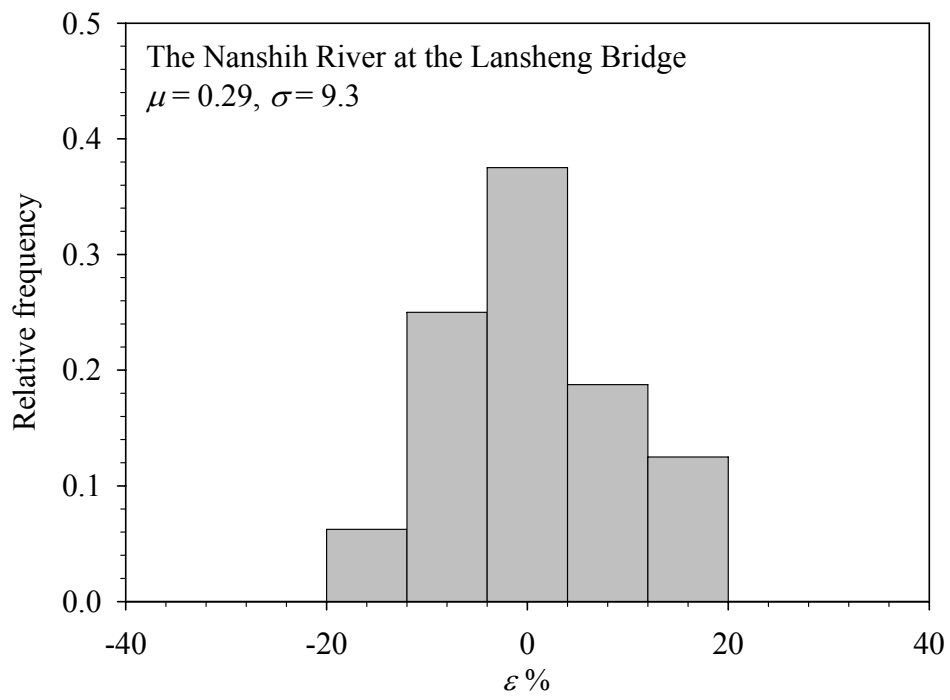


(a)

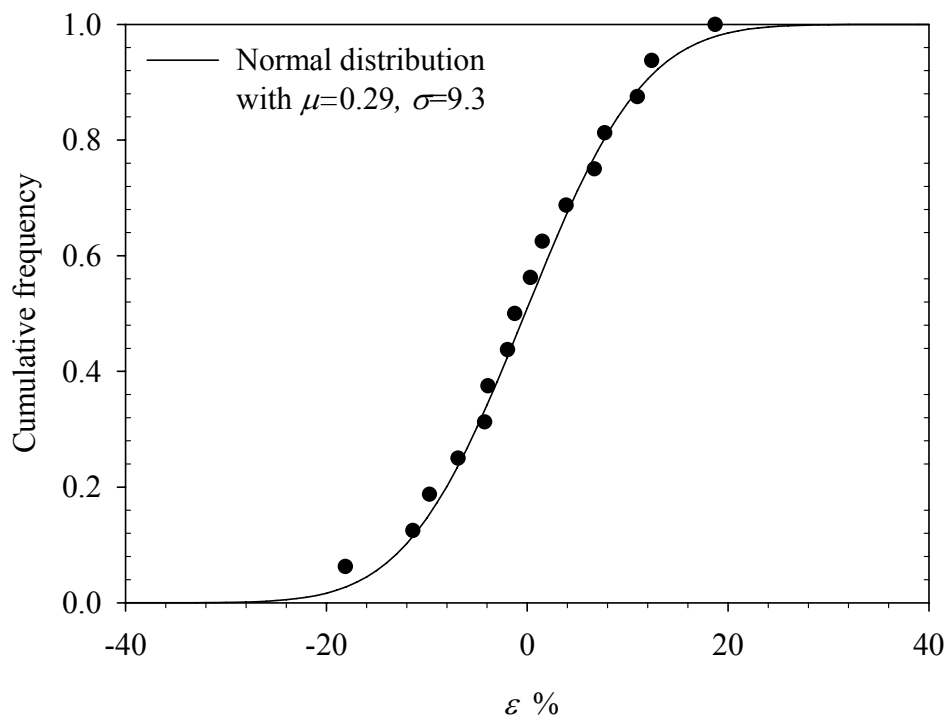


(b)

Fig. 10. Accuracy of estimated discharge in the Nanshih River at the Lansheng Bridge; (a) Calibration; (b) Validation.



(a)



(b)

Fig. 11. Frequency functions for a normal distribution fitted to error %; (a) Relative frequency of error %; (b) Cumulative frequency of error %.

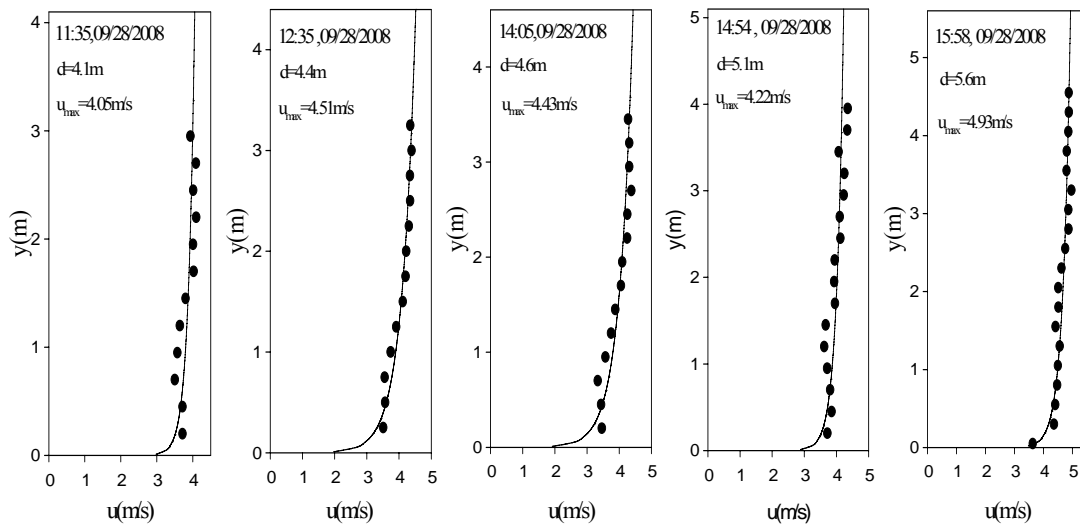


Fig. 12. Velocity distribution on y -axis during Typhoon Jangmi in 2008.

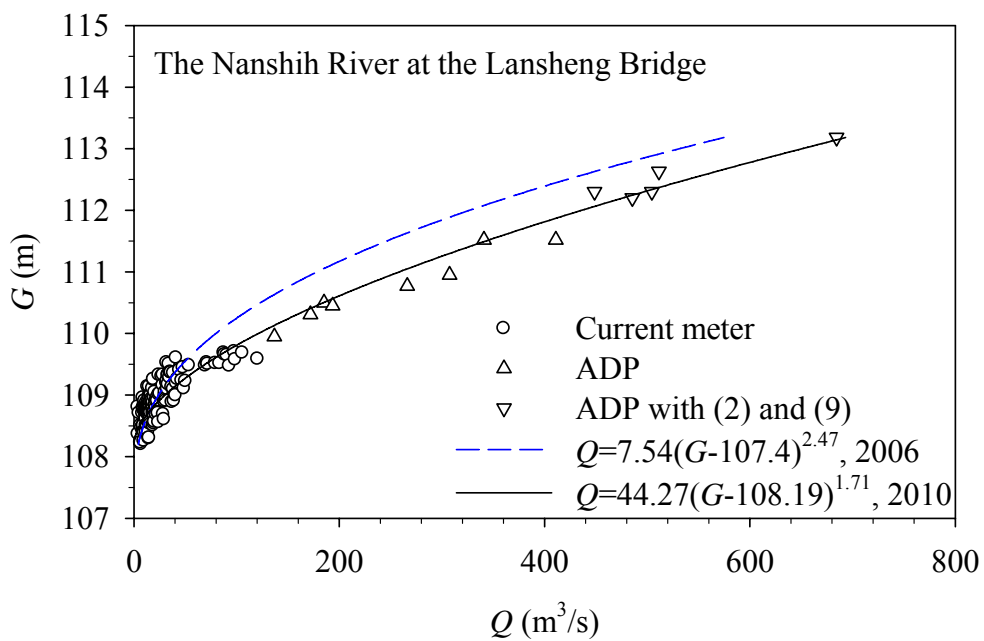


Fig. 13. Stage-discharge rating curve of the Nanshih River at the Lansheng Bridge.